MICCAI 2025 | September 23–27, 2025 | Shape in Medical Imaging Workshop | Daejeon, Korea | Paper #0023

ARTIFICIAL INTELLIGENCE PRECISION HEALTH INSTITUTE
UNIVERSITY OF HAWAI'I

Deep Learning Enables Large-Scale Shape and Appearance Modeling in Total-Body DXA Imaging

Connect with me!

Arianna Bunnell[1,2], Devon Cataldi[1], Yannik Glaser[2], Thomas K. Wolfgruber[1], Steven Heymsfield[3], Alan B. Zonderman[4], Thomas L. Kelly[5], Peter Sadowski[2], and John A. Shepherd[1]
[1]University of Hawai'i Cancer Center, [2]University of Hawai'i at Mānoa, [3]Pennington Biomedical Research Center, [4]NIA/NIH/IRP, [5]Hologic, Inc.

Read the paper!

Introduction

- Total-body dual X-ray absorptiometry (TBDXA) represents a relatively low- cost whole-body imaging modality with low levels of radiation exposure acceptable for use in longitudinal studies [1].
- Shape and Appearance Modeling (SAM) has been used extensively for the modeling of shape and texture in medical imaging [2–4].
- A challenge limiting the adoption of SAM for studying the variance of shape in medical imaging is that it requires trained annotators to place fiducial points on all images. This makes preparation a costly and time-consuming endeavor for even small datasets.
- In this work, we develop an accurate method for automated point placement to facilitate the use of SAM on larger TBDXA datasets.
- We demonstrate an example application of this method to several large NIH TBDXA datasets and explore the association of body shape and appearance SAM features with health markers.

Methods

- TBDXA images were collected from five different studies: the HABC study [5]; the MrOS study [6]; the SUA study [7]; the HANDLS study [8]; SUK study [9]; and the MEC study [10].
- See **Table 1** for a breakdown of study populations and data splits for SAM. HANDLS was used to test association of discovered SAM features with biomarkers in a completely independent sample
- We defined 105 bony and soft tissue fiducial points. See **Figure 1.**
- We finetune a DeepPose [11] model with a ResNet-101 [12] backbone pretrained on MS-COCO [13] for point placement from expert point annotations.
- SAM and display functions were done in C++ using the UoMApM software [14] with automatically-placed points. See **Figure 1** for a procedural breakdown of the SAM method.
- For health marker, the 10th and 90th percentiles of that marker were identified in the HANDLS and HABC testing datasets. A two-sample Kolmogorov-Smirnov [15] test was performed to investigate if SAM features were identically distributed at the tails of the health marker distributions. Spearman correlations were also computed.

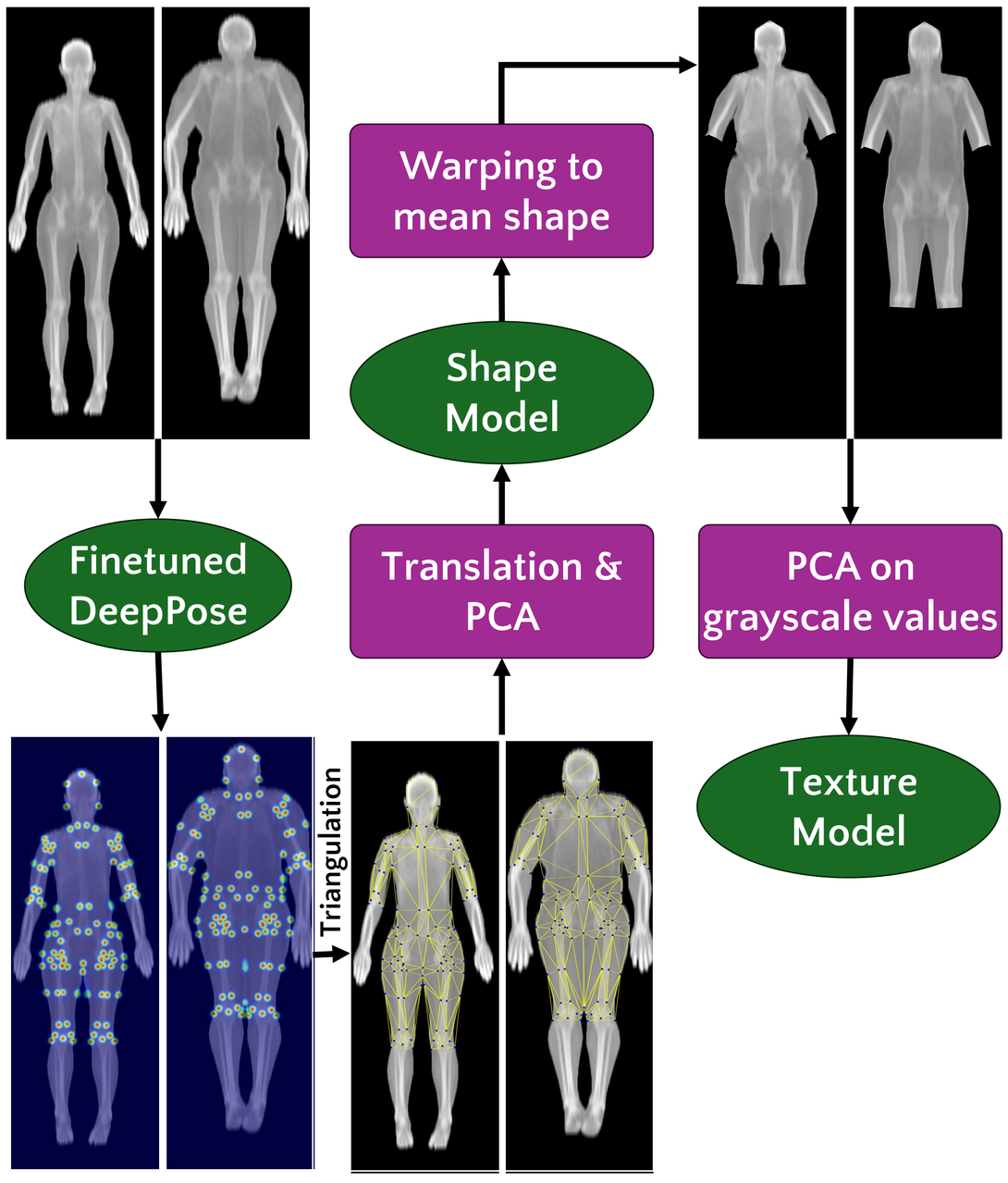

Figure 1: An overview of the complete SAM process. First, points are automatically placed on the images using our finetuned DeepPose model. Then, triangulation files are applied. PCA is done first on the points (shape model) then on the interior grayscale values (texture model). **Purple** represents UoMApM tools. **Green** represents our contributions.

		Participants, N		TBDXA scans, N		Mean age, years (SD)	Mean scans/person, N (SD)	Mean BMI, kg/cm² (SD)
		Female	Male	Female	Male			
Training	Overall	1,881	7,716	7,810	18,652	74.5 (6.2)	2.8 (2.1)	27.2 (4.5)
	HABC	1,255	1,148	7,181	6,436	75.3 (3.0)	5.7 (2.2)	27.2 (4.8)
	MEC	395	438	395	438	69.7 (2.8)	1.0 (0.0)	28.1 (5.0)
	MrOS	0	5,939	0	11,587	75.1 (5.8)	2.0 (0.7)	27.3 (3.8)
	SUA	231	191	234	191	45.2 (16.1)	1.0 (0.1)	27.0 (6.6)
Testing	Overall	1,819	1,436	5,241	4,222	62.6 (12.6)	2.91 (1.8)	29.3 (6.9)
	HABC	318	321	1,809	1,793	75.2 (3.0)	5.64 (2.2)	27.1 (4.7)
	HANDLS	1,499	1,113	3,432	2,429	54.9 (9.6)	2.24 (0.9)	30.7 (7.7)

Table 1: Scan- and patient-level counts for the SAM training and testing samples.

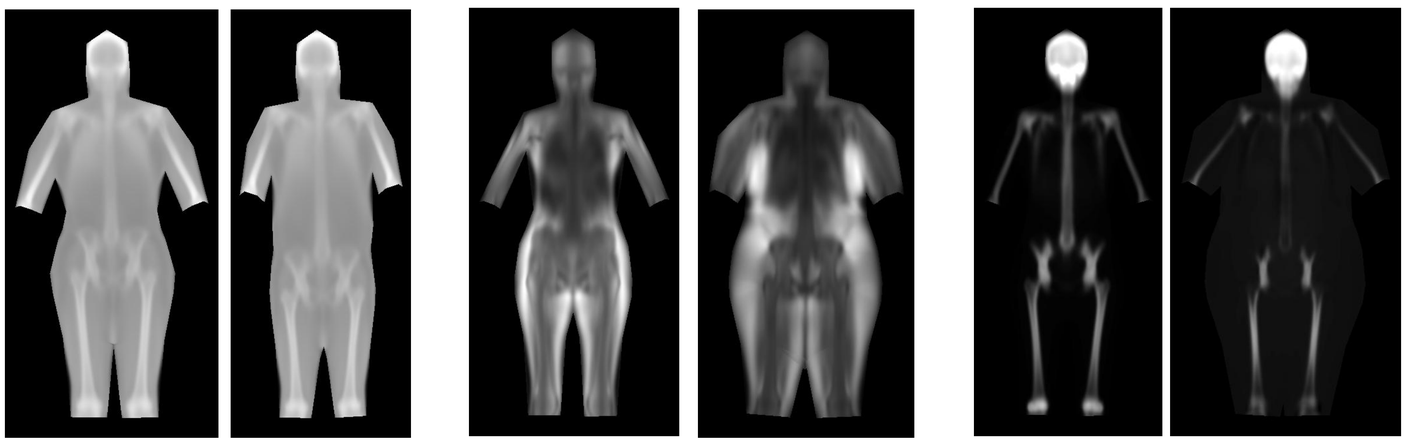

HDL ratio (HANDLS) `air ratio` | Blood glucose (HABC) `d fat` | Calcium (HANDLS) `bmd irs`

Figure 2: Reconstructed images from the 10th (left) and 90th (right) percentiles for appearance SAM features found to be significantly differently distributed via Kolmogorov-Smirnov tests. Reconstructions are male (left), female (middle), and female (right).

Results

- Point placement results from the finetuned DeepPose model on 500 scans from the external HABC dataset as compared to the expert-annotated points were: 99.5% Percentage Correct Keypoints, 8.49 End Point Error, and 0.007 Normalized Mean Error.
- We found that 29 shape modes explained 95% of the shape variance for males and 28 shape modes explained 95% of the shape variance for females.
- We found that most health markers – fasted blood glucose, hemoglobin A1c, grip strength, and walk speed – showed weak association with the first 5 SAM features..
- **Figure 2** shows reconstructed SAM modes for HDL ratio (cardiometabolic marker), blood glucose (metabolic), and calcium (cardiometabolic), all found to be significant via KS tests. Images are built by taking the feature mean at the 10th and 90th percentile if significant, or over the entire dataset if not, and transforming back to image space.
- Glucose and insulin-related health markers were found to be significantly differently distributed in both the HANDLS and HABC cohorts,

Conclusion

- Our automated placement of fiducial markers shows human-level performance and enables us to systematically annotate TBDXA images for SAM building. This enables hypothesis building and data-driven discovery on large-scale TBDXA data.
- The limitations of this work are a lack of consistent health markers, limiting cross-study analyses; a large difference in the age composition; and lack of longitudinal analysis.
- Future work may use a more comprehensive method for pose alignment and recruitment of participants prospectively to quantify metabolic panel accuracy.

References

[1] Blake, G.M., M. Naeem, and M. Boutros, Comparison of effective dose to children and adults from dual X-ray absorptiometry examinations. Bone. 38(6): p. 935-942 (2006). [2] Cootes, T.F. and C.J. Taylor. Statistical models of appearance for medical image analysis and computer vision. Medical Imaging 2001: Image Processing. 2001. SPIE. [3] Cootes, T.F., et al., Use of active shape models for locating structures in medical images. Image and vision computing. 12(6): p. 355-365 (1994). [4] Patenaude, B., et al., A Bayesian model of shape and appearance for subcortical brain segmentation. Neuroimage. 56(3): p. 907-922 (2011). [5] Newman, A.B., et al., Strength and muscle quality in a well-functioning cohort of older adults: the Health, Aging and Body Composition Study. Journal of the American Geriatrics Society. 51(3): p. 323-330 (2003). [6] Orwoll, E., et al., Design and baseline characteristics of the osteoporotic fractures in men (MrOS) study—a large observational study of the determinants of fracture in older men. Contemporary clinical trials. 26(5): p. 569-585 (2005). [7] Ng, B.K., et al., Detailed 3-dimensional body shape features predict body composition, blood metabolites, and functional strength: the Shape Up! studies. The American journal of clinical nutrition. 110(6): p. 1316-1326 (2019). [8] Evans, M.K., et al., Healthy aging in neighborhoods of diversity across the life span (HANDLS): overcoming barriers to implementing a longitudinal, epidemiologic, urban study of health, race, and socioeconomic status. Ethnicity & disease. 20(3): p. 267 (2010). [9] Kalkwarf, H.J., et al., The bone mineral density in childhood study: bone mineral content and density according to age, sex, and race. The journal of clinical endocrinology & metabolism. 92(6): p. 2087-2099 (2007). [10] Kolonel, L.N., et al., A multiethnic cohort in Hawaii and Los Angeles: baseline characteristics. American journal of epidemiology. 151(4): p. 346-357 (2000). [11] Toshev, A. and C. Szegedy. Deeppose: Human pose estimation via deep neural networks. Proceedings of the IEEE conference on computer vision and pattern recognition. 2014. [12] He, K., et al. Deep residual learning for image recognition. Proceedings of the IEEE conference on computer vision and pattern recognition. 2016. [13] Lin, T.-Y., et al., Microsoft COCO: Common Objects in Context, in Computer Vision – ECCV 2014. 2014, Springer International Publishing. p. 740-755. [14] Cootes, T.F., University of Manchester Appearance Model Library and Tools. 2024. [15] Massey Jr, F.J., The Kolmogorov-Smirnov test for goodness of fit. Journal of the American statistical Association. 46(253): p. 68-78 (1951).